

Electrical Stress Monitoring of Distribution Transformers using Bushing Embedded Capacitive Voltage Dividers and Rogowski Coils

Fulufhelo Andrew Netshiongolwe and John Michael van Coller

Abstract-- Premature failure of distribution transformers has prompted the need to measure the electrical stresses that may be causing such failures. This paper presents a non-intrusive alternative means of monitoring electrical stresses on the medium voltage (MV) side of distribution transformers rated 16 kVA up to 2 MVA with the aim of curbing premature transformer failure. An electric field control screen embedded in a 24 kV bushing is used to form a capacitive voltage divider measuring both power frequency and transient voltages. A shielded Rogowski coil placed around the bushing screen measures both power frequency and transient currents. Simulation models are able to recreate the laboratory measured results.

Keywords: Rogowski coil, impulse currents, impulse voltage, capacitive voltage divider, Smart Grids

I. INTRODUCTION

The presence of transients, harmonics, ever increasing changes in loads and load profiles increases the electrical stresses experienced by transformers at the distribution level. Due to the low capital cost of distribution transformers, minimal condition monitoring is installed. Colour coded thermal stickers that require field inspection are currently used for overload monitoring on Eskom distribution transformers rated up to 2 MVA [1]. The increase in the premature failures of these transformers has prompted the need to seek alternative monitoring techniques.

The introduction of Smart Grids affords utilities the ability to better manage load profiles, monitor and manage electrical stresses and improve electrical equipment availability [2]. This research focuses on the development of a low cost bushing with embedded current and voltage transducers capable of monitoring wideband electrical stresses on the MV side of distribution transformers. The operating principle of the designed bushing capacitive voltage divider and Rogowski coil is given. Various tests were performed to evaluate the performance of the designed bushing against commercially available current and voltage probes. A comparison between simulated and measured results is also presented.

This work was funded by Eskom through the Eskom Power Plant Engineering Institute (EPPEI) program. F.A. Netshiongolwe is with Eskom Generation and is studying towards an MSc in Electrical Engineering at the University of the Witwatersrand (e-mail: netshifa@eskom.co.za). J. M. Van Coller is with the University of Witwatersrand and is a Senior Lecturer who has been with University for many years and holds the Eskom Chair of High Voltage (e-mail: john.vancoller@wits.ac.za).

Paper submitted to the International Conference on Power Systems Transients (IPST2015) in Cavtat, Croatia June 15-18, 2015

II. BACKGROUND

A. Electrical stress monitoring

Premature failure of distribution transformers may be caused by unmonitored transient and power frequency electrical stresses. Current and voltage monitoring on the low voltage (LV) side of pole-mount transformers within Eskom distribution networks has led to the identification of transformers that are subjected to stresses that include overloading, severe load unbalances and overcurrent conditions [3]. Such findings prompted the need to develop low cost electrical transducers that could be used to identify other electrical stresses that could lead to premature transformer failure. Another example is where failed surge arresters allow large transient voltages to appear across transformers which may result in their premature failure [4]. The presence of harmonics introduced by the increased use of nonlinear loads increases the risk of transformer over-temperatures [5].

In this study, focus is on the development of low cost electrical stress monitoring sensors suitable for use on the medium voltage (MV) side of distribution transformers. Information obtained from such sensors can then be used to identify transformers that are exposed to excessive electrical stresses that may lead to premature failure.

B. Rogowski coil current sensor

Rogowski coils with a non-magnetic core, such as the one depicted in Fig.1, have been shown to have the following superior features [6]-[8]:

- High bandwidth (suitable for transients)
- Multiple primary current measurement ranges
- Non-intrusive to the primary circuit
- Modular in size
- Linear

The Rogowski coil output voltage is a function of the time derivative of the measured primary current. The coil output voltage based on the properties in Fig. 1 and Table 1 is given by [6], [8]:

$$V_c = -\frac{d\phi}{dt} = -\mu_0 N A \frac{di}{dt} = -M \frac{di}{dt} \quad (1)$$

-where:

V_c is the coil output voltage [V]

ϕ is the coil flux linkage [Weber-turns]

μ_0 is the permeability of free space [$4\pi \times 10^{-7}$ H/m]

N is the number of turns
A is the coil area [m²]
i is the current in the primary conductor [A]
M is the mutual inductance [H]

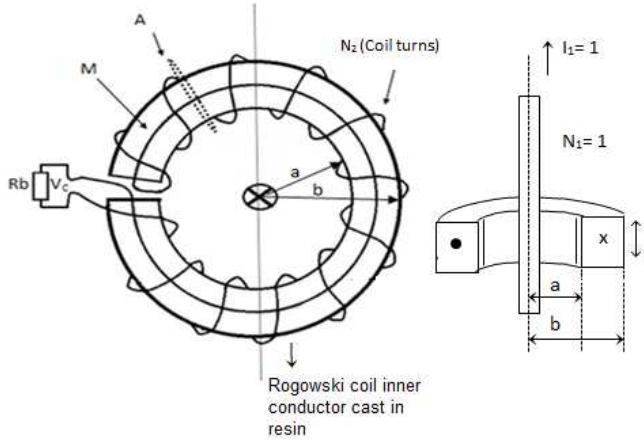


Fig. 1. Rogowski coil cast in resin

TABLE 1
DESIGNED ROGOWSKI COIL SPECIFICATION

Parameter	Description	Value
d_w [mm]	Wire diameter	0.25
R [Ω]	Wire resistance	18.5
a [mm]	Inner radius	40
b [mm]	Outer radius	60
h [mm]	Coil height	20
l [mm]	Core length	390
A [mm ²]	Coil area	400
N_2	Number of turns	668

A widely accepted lumped parameter model for the Rogowski coil is shown in Fig. 2 below. The calculated mutual inductance of the Rogowski coil with properties in Table 1 and Fig. 1 is given by [9]:

$$M = \frac{\mu_0 N_2}{2\pi} h \ln\left(\frac{b}{a}\right) \quad (2)$$

The corresponding self-inductance is given by:

$$L = \frac{\mu_0 N_2^2}{2\pi} h \ln\left(\frac{b}{a}\right) \quad (3)$$

The coil lumped capacitance is given by:

$$C = \frac{2\pi^2 \epsilon^2 (a+b)}{\log[(a+b)/(b-a)]} \quad (4)$$

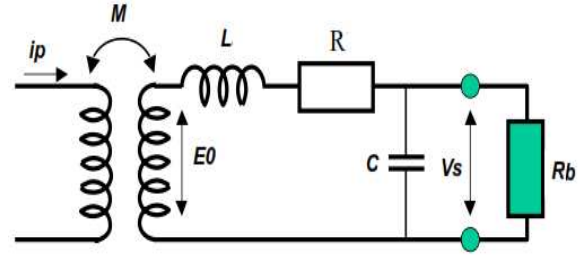


Fig. 2. Rogowski coil electrical model [6]

TABLE 2
CALCULATED COIL PARAMETERS

Parameter	Description	Value
M (nH)	Mutual Inductance	861
L (mH)	Coil self-inductance	2.17
C (pF)	Coil capacitance	50.2

Calculated coil parameters have been shown to differ from the measured parameters at high frequencies. Because of this, the decision was made to rather base the model on measurements. Hashmi et al used coil parameters measured at 1 kHz to simulate Rogowski coil behavior whilst measuring partial discharges [10]. Shafiq et al. developed a parameter identification method that involves measuring impulse waveforms with a Rogowski coil whose output is sensed with the use of a differential probe [11]. A Fast Fourier transform of the output of the differential probe was then used to find the resonant frequencies for different configurations. The resonant frequencies were then used to determine the relationship between the inductances and capacitances of the coil.

In this study a 20 MHz function generator, an oscilloscope and tank circuits were used to determine the coil parameters using the resonance frequency calculations given in (5)-(10) below. The output of the function generator is applied across a resistor in series with a coil that is in parallel with a known capacitor C_T . The measured voltage across the coil reaches a peak at the point of resonance where the relationship between the total circuit capacitance and the inductance is given by:

$$F_r = \frac{1}{\sqrt{L_T(C_m + C_p + C_T)}} \quad (5)$$

- where:

F_r is the tank circuit resonant frequency [Hz]

L_m is the coil inductance [H]

C_m is the coil stray capacitance [F]

C_p is the probe capacitance [F]

C_T is the capacitance of the known capacitor [F]

Based on (5), given the capacitance of the known capacitor 1, C_{T1} , which gives a measured tank resonant frequency F_{r1} when combined with the designed coil, (5) can be rearranged such that:

$$F_{r1}^2 L_m (C_p + C_m + C_{T1}) = 1 \quad (6)$$

For the capacitance of the known capacitance 2, C_{T2} , and

measured tank resonant frequency, F_{r2} , the above equation becomes:

$$F_{r2}^2 L_m (C_p + C_m + C_{T2}) = 1 \quad (7)$$

Taking a ratio of (6) and (7) results in the following expression:

$$(C_p + C_m + C_{T1}) = \frac{F_{r1}^2}{F_{r2}^2} (C_p + C_m + C_{T2}) \quad (8)$$

From the above expression the coil stray capacitance and probe capacitance are given by:

$$C_m + C_p = \frac{C_{T2} \left(\frac{F_{r1}^2}{F_{r2}^2} \right) - C_{T1}}{1 - \frac{F_{r1}^2}{F_{r2}^2}} \quad (9)$$

Shafiq et al suggest taking other measurements with two probes in order to determine the probe capacitance [6]. The above expression is then modified such that:

$$C_m + 2C_p = \frac{C_{T2} \left(\frac{F_{r21}^2}{F_{r22}^2} \right) - C_{T1}}{1 - \frac{F_{r21}^2}{F_{r22}^2}} \quad (10)$$

- where F_{r21} and F_{r22} are the new resonance frequencies that result due to the additional probe capacitance. The probe capacitance is calculated by subtracting the value obtained from (9) from that obtained from (10). Once the probe capacitance is calculated, the coil capacitance is then obtained from (9). The coil inductance is found by averaging the calculated inductance at the different resonance frequencies above. Table 2 gives all the corresponding measured and calculated coil parameters of the designed Rogowski coils. The accuracy of both measured and calculated parameters in modelling the designed Rogowski coils performance is evaluated by comparing simulated and measured results in the subsequent sections.

TABLE 3
MEASURED COIL PARAMETERS

Parameter	Parameter	Value
C_{T1} [pF]	Tank known capacitance 1	11
C_{T2} [pF]	Tank known capacitance 2	56.25
F_{r1} [kHz]	Resonance frequency ($C_{T1} + C_p$)	480
F_{r2} [kHz]	Resonance frequency ($C_{T2} + C_p$)	397
F_{r21} [kHz]	Resonance frequency ($C_{T1} + 2C_p$)	405
F_{r22} [kHz]	Resonance frequency ($C_{T1} + 2C_p$)	326
C_p [pF]	Probe capacitance	8
C_m [pF]	Coil capacitance	4.1
L_m [mH]	Coil inductance	5.37
M [nH]	Mutual Inductance	510

C. Voltage monitoring using bushing screen

Non-condenser bushings such as cast resin MV bushings are subjected to both axial and radial stresses. High axial stresses may lead to surface tracking [12]. The presence of high radial stresses may lead to partial discharges or even insulation breakdown [13]. In this study the bushing screen is used for electric field stress control as well as voltage measurement. The designed bushing consists of one screen surrounding the bushing conductor. This screen is connected to an external capacitor to form a capacitive voltage divider. The insulation between the screen and the bushing conductor can be represented by a resistor in parallel with a capacitor as shown in Fig. 3. The position of the screen in relation to the bushing conductor suggests a cylindrical geometry. The insulation capacitance between the conductor with reference to Fig 3 and Table 4 parameters is given by Kuffel et al. [14]:

$$C_1 = \frac{2\pi\epsilon_0\epsilon_r' h}{\ln \frac{b}{a}} \quad [\text{F/m}] \quad (11)$$

The corresponding insulation resistance at angular frequency ω is given by:

$$R_1 = \frac{\ln \frac{b}{a}}{w 2\pi\epsilon_0\epsilon_r''} \quad [\Omega/\text{m}] \quad (12)$$

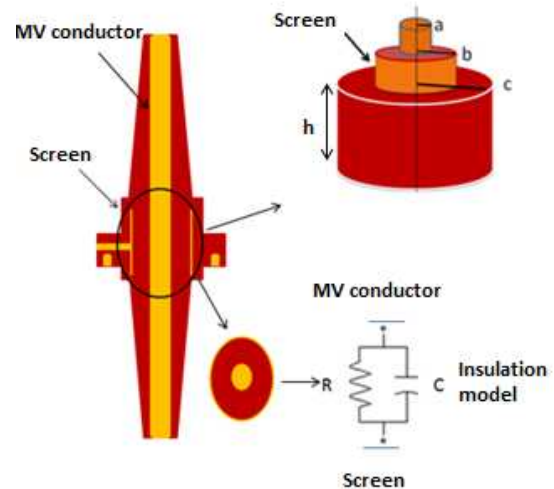


Fig. 3. Cross-section of a screened 24 kV epoxy resin bushing with emphasis on the position of the screen relative to the bushing conductor

The dielectric resistance at power frequency is large enough such that the measured bushing voltage is given by:

$$V_{out} = \frac{C_1}{C_1 + C_2} V_{in} \quad (13)$$

- where:

- C_1 is the capacitance between the bushing screen and the bushing conductor [F]
- C_2 is the capacitance of the external capacitor [F]
- V_{in} is the input voltage [V]

V_{out} is the output voltage [V]

TABLE 4
EPOXY RESIN 24 kV BUSHING PARAMETERS

Parameter	Parameter description	Value
ϵ_0 (F/m)	Free space permittivity	8.854E-12
ϵ'_r	Relative permeability	3.8
ϵ''_r	Relative permeability	0.038
Tan delta	Epoxy resin tan delta	0.01
a(mm)	Conductor radius	6
b (mm)	Screen radius	30
h (mm)	Screen height	60

The measured capacitance between the bushing screen and the bushing conductor was 22.23 pF. The capacitance of the external capacitor connected between the bushing screen and the external earth was 47 nF. Based on (13), the voltage division ratio was calculated as 2115:1. A different voltage division ratio can be obtained by using a different external capacitor C_2 .

III. EXPERIMENTAL SETUP

The designed bushing was subjected to a voltage impulse corresponding to its rated BIL of 150 kV. The designed bushing was coated with silicone rubber to improve its pollution performance [15]. Other tests included wet and dry power frequency withstand tests as described in SANS/IEC 60137 [16]. The designed bushing did not puncture or flashover when these tests were performed. The experimental setup for tests related to the performance of the embedded Rogowski coil and the capacitive voltage divider are described below.

A. Power frequency current measurement

The designed bushing was tested with a high power frequency current source as shown in Fig. 4 below. The current flowing through the bushing was varied using the variac. The measured current value was compared with that obtained using a 100/1 commercial wideband current probe. Currents were varied up to the 250 A rating of the bushing. Further measurements were made at 160% of the rated current.

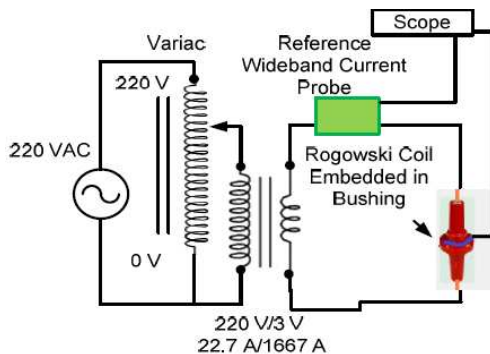


Fig. 4. Power frequency current measurements

B. Impulse current measurements

An 8/20 μ s current impulse generator shown in Fig 5 was used to generate current impulses that were passed through the designed bushing. The measured current value was compared with that obtained using the same 100/1 commercial wideband current probe. Impulse currents of different amplitudes were obtained by varying the input AC source voltage which charged the capacitors to the desired level before discharging the current impulse through the bushing.

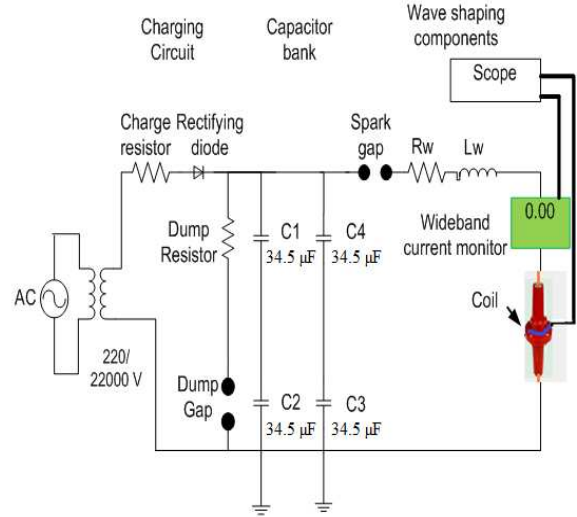


Fig. 5. Impulse current measurements circuit

C. Power frequency voltage measurement

Power frequency voltage measurements were performed by connecting the designed bushing to the output of a 0.22/60 kV transformer on the high voltage side. The output voltage of the transformer was varied using the variac as shown in Fig. 6. The measured voltage from the bushing capacitive voltage divider was compared with that obtained using a commercially available 1000/1 capacitive voltage probe.

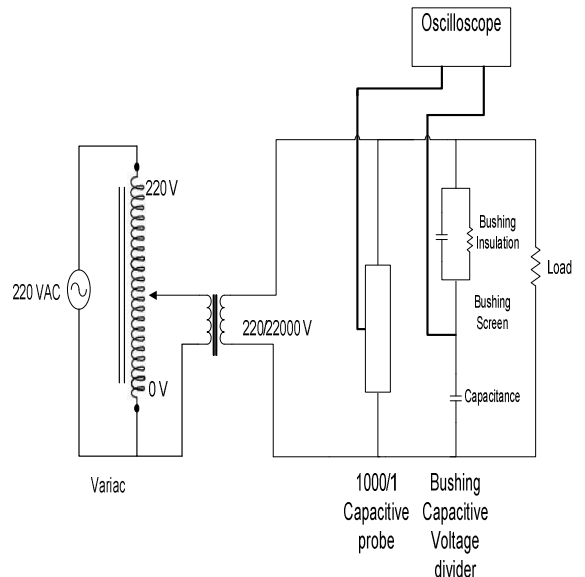


Fig. 6. Power frequency voltage measurement

D. Impulse voltage measurement

An 8 stage 1.2/50 μs voltage impulse generator was used to generate impulse voltages that were applied on the bushing. The bushing was subjected to voltages up to the rated BIL of 150 kV. The output of the bushing divider was compared to that of a wideband resistive divider. Each of the measured impulses were adjusted using correction factors as prescribed in SANS/IEC 60060-1[17].



Fig. 7. Impulse voltage measurement setup

IV. SIMULATION AND MEASURED RESULTS

An accurate simulation model is required since this allows compensation to be designed for any observed nonlinearity. Simulation models of the current and voltage sensors were developed using the simulation package ATPDraw.

A. Current measurements

Several authors have used the modified version of the ATPDraw saturable transformer model in the simulation model of Rogowski coils [8, 10]. This is achieved by modifying the non-linear saturable transformer flux versus current relationship such that it becomes linear as depicted in Fig. 8. In this study the parameters found in Tables 2 and 3 were used to develop the simulation model that reproduced the laboratory measured results. The accurately measured impulse currents were used as input currents to the circuit model shown in Fig 9. A 10/1 passive voltage probe was used as an interconnection between the oscilloscope and the Rogowski coil.

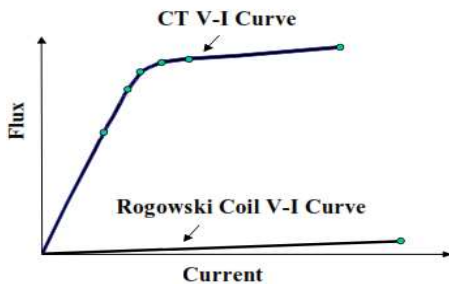


Fig. 8 Transformation of ATPDraw saturable transformer model to a Rogowski coil model [8]

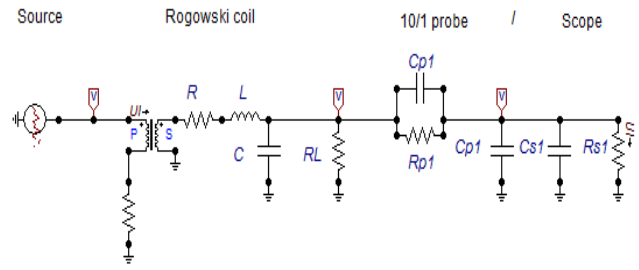


Fig. 9. Simulated current measurement circuit

A comparison between the unintegrated output of the Rogowski coil and the simulated behaviour is shown in Fig. 10. The measured Rogowski coil output voltage waveform is consistent with the voltage waveform obtained by [18]. The results were obtained whilst measuring an 6 kA 8/20 μs current impulse shown in Fig. 11 below. The simulated behaviour based on measured parameters closely approximated the measured unintegrated output of the Rogowski coil. Calculated parameters based on the physical properties result in an overestimation of the coil output. The numerically integrated output of the Rogowski coil shown in Fig. 11 closely approximates the measured impulse waveform. Observed results when measuring 9 kA and 15 kA current impulses remain consistent with the behaviour illustrated in Fig. 10 and Fig. 11.

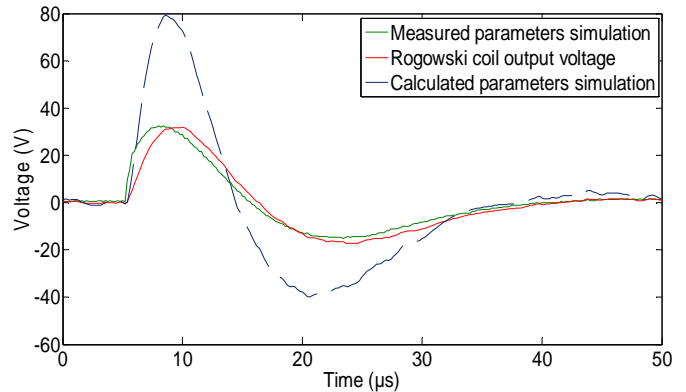


Fig. 10 Comparison between the designed Rogowski coil measured output voltage and the simulated output voltage

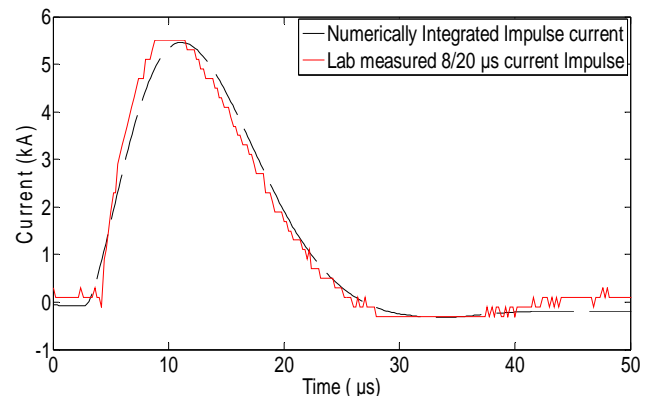


Fig. 11. Comparison between 6 kA wideband current probe measurement with the numerically integrated Rogowski coil

output voltage.

The output of the designed Rogowski coil when measuring rated 50 Hz current is shown in Fig. 12. The unintegrated current is 90 degrees out of phase with the output of a commercial wideband probe as shown in Fig. 13 – as expected.

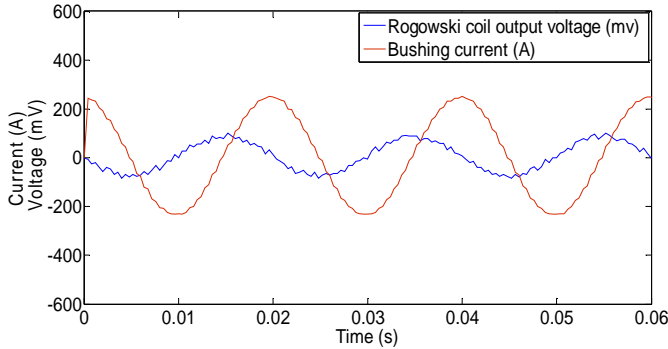


Fig. 12. Performance of the Rogowski coil whilst measuring rated current

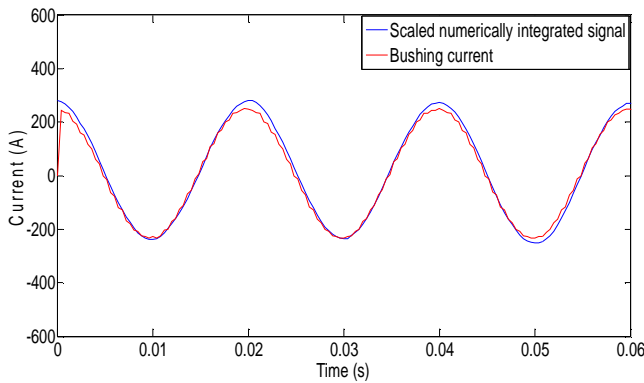


Fig. 13. Scaled numerically integrated output of the designed Rogowski coil

B. Voltage measurements

The output of the bushing capacitive voltage divider was observed to offer linear results comparable with that of a commercial capacitive voltage probe when measuring 50 Hz power frequency voltages. Observed results were measurable from 1 kV upwards. They were also consistent with the calculated 2115:1 transformation ratio. Fig. 14 shows the measurements that were taken at 2 kV and Fig. 15 shows those taken at 24 kV.

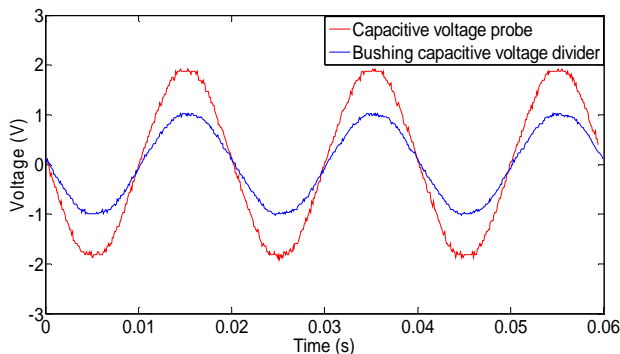


Fig. 14 Low voltage measurements

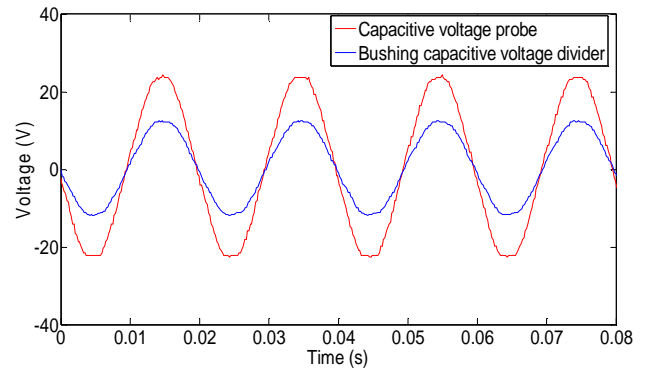


Fig. 15. High voltage measurement

When measuring impulse voltages, nonlinearity was observed when measuring impulse voltages larger than 60 kV. This nonlinearity was also found with other capacitive dividers that used epoxy resin as a dielectric. This behaviour suggested a simulation model as shown in Figure 16 below

The ATPdraw nonlinear type 92 resistor was used to simulate the nonlinearities introduced by the epoxy resin dielectric when subjected to impulses larger than 60 kV. The non-linear resistor current versus voltage characteristic was chosen to give good results for a 130 kV voltage impulse. Fig. 17 to 19 show comparisons between the simulated and measured voltage impulses using the model with the optimized non-linear resistor and those without.

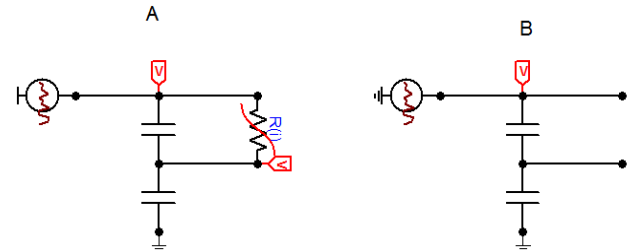


Fig. 16. Simulated bushing capacitive voltage divider model.

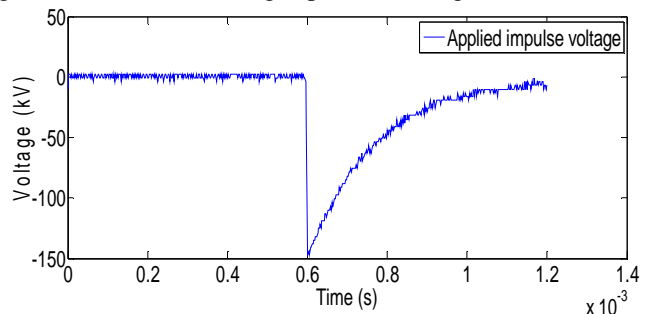


Fig. 17. Applied rated BIL 150 kV 1.2/50 μ s impulse voltage

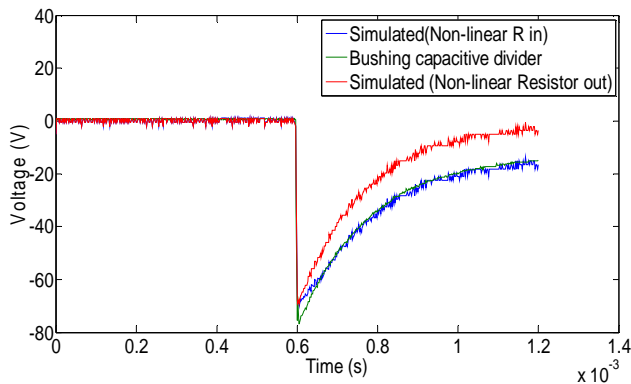


Fig. 18. Bushing capacitive voltage divider output at the rated BIL

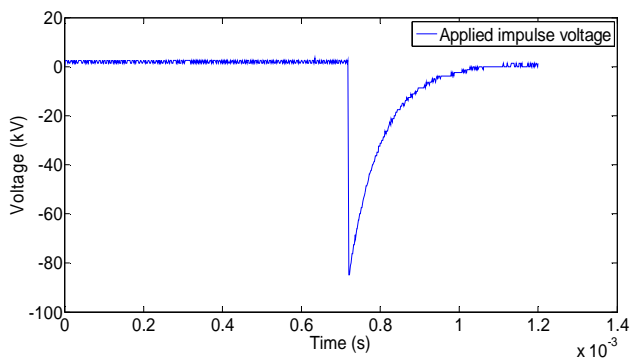


Fig. 19. Applied 80 kV 1.2/50 μ s impulse voltage

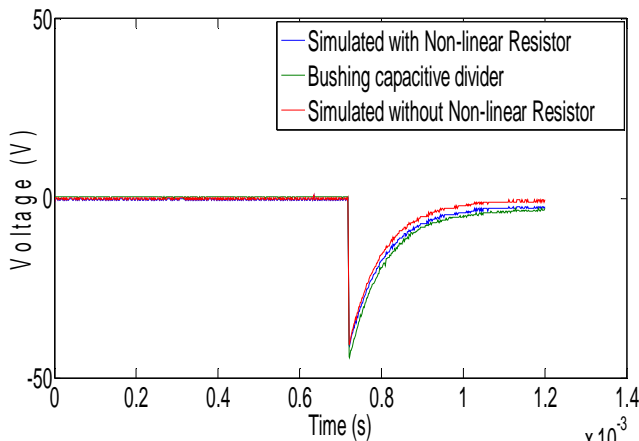


Fig. 20. Bushing capacitive voltage divider output for the applied 80 kV 1.2/50 μ s impulse voltage

V. INDUSTRY BENEFITS

The study conducted showed the possibility of using a low cost screen-based bushing capacitive voltage divider and a bushing embedded Rogowski coil for performing MV side measurements. These transducers can be used for identifying transformers that are subjected to severe electrical stresses on the MV side and thus can help in the prevention of premature transformer failure. With refined sensitivity of the designed Rogowski coils, the bushing with embedded voltage and current probes can assist in reducing costs associated with the measurements required for implementing the Smart Grid of the future.

VI. CONCLUSION

This paper presented the design, testing and modelling of an MV transformer bushing with embedded voltage and current probes for use with distribution transformers. Simulated results obtained using measured parameters were consistent with laboratory measured results for both power frequency and impulse current measurements. Power frequency voltage measurements using the bushing capacitive voltage divider showed a constant 2115:1 voltage transformation ratio for the range 1 kV up to 24 kV. Observations showed nonlinearities when 1.2/50 μ s impulses with magnitude larger than 60 kV were applied. With an accurate nonlinear model of this behaviour, a compensation circuit can be designed to cancel out this non-linearity.

VII. REFERENCES

- [1] Distribution Guide– Part 1: Network Planning Guideline for Transformers, Eskom Guideline 34-542, Nov. 2010.
- [2] C. G.Elsworth, *The Smart Grid and Electric Power Transmission*, Nova Science Pub. Incorporated, 2008, p1-45.
- [3] R Kleinhans, “Current and Voltage Monitors Combat Theft and Improve Supply Quality”, *Energize: Transmission and Distribution*, pp. 41-45. Sep. 2011.
- [4] W. J. D. van Schalkwyk and J. van Coller, “An Investigation into a More Optimal Choice of BIL on MV Feeders”, in *2013 Proc.Cigré 7th South African Regional Conf.*
- [5] M. Sharengi, B. Phung, M. Naderi, T. Blackburn and E. Anbikairajar, “Effects of Current and Voltage Harmonics on Distribution Transformer Losses”, in *2012 Proc. International Conf. on Condition Monitoring and Diagnosis(CMD)*, Bali, pp. 633-636, 2012
- [6] *IEEE Guide for the Application of Rogowski Coils Used for Protective Relaying Purposes*, IEEE Standard C37.235, Sep. 2007.
- [7] W. F. Ray and R .M. Davis, “High frequency improvements in wide bandwidth Rogowski transducers”, in *1999 Proc. EPE 99 Conf.*
- [8] L. A. Kojovic. “Rogowski Coil Transient Performance and ATP Simulations for Applications in Protective Relaying”, in *2005 Proc. International Conf. on Power Systems Transients International (IPST’05)*.
- [9] M. Argueso , G. Robles and J. Sanz, "Implementation of a Rogowski coil for the measurement of partial discharges", *Rev. Sci. Instrum.*, vol. 76, no. 6, pp. 065107-1 -065107-7, May 2005.
- [10] G. M. Hashmi, M. Lehtonen, and M. Nordman, “Modeling and Experimental Verification of On-line PD Detection in MV Covered-conductor Overhead Networks”, *IEEE Transaction on Dielectrics and Electrical Insulation*, vol. 17, Issue 1, pp. 167-180, Feb 2010.
- [11] M Shafiq, G. Amjad Hussain, L Kütt and M Lehtonen. “Effect of geometrical parameters on high frequency performance of Rogowski coil for partial discharge

- measurements." *Measurement* (49), pp. 126-137, 2014.
- [12] M. H. Ryan, *High Voltage Engineering and Testing*, 2nd ed., IET Publications, 2001, pp. 405-430.
- [13] H. Ilias, M. A. Tunio, A. H. A. Bakar and H. Mokhlis, "Distribution of Electric Field in Capacitor and Surge Arrester Bushings" in *2012 Proc. IEEE International Conf. on Power and Energy (PECon)*, pp. 461-466. (2012)
- [14] E. Kuffel, W. S. Zaengle and J. Kuffel, *High Voltage Engineering- Fundamentals*, Butterworth-Heinemann, 2nd ed., 2000
pp. 201-241.
- [15] W. L. Vosloo, R. E. Macey and C. de Tourreil, *The Practical Guide to Outdoor High Voltage Insulators*, Crown Publications, Sep 2006, pp. 186-187
- [16] Insulated Bushings for Alternating Voltages Above 1 000 V, SANS Standard 60137, ed. 3, 2010.
- [17] High voltage tests: Atmospheric correction factors, SANS Standard 60060-1, 1989.
- [18] K. Schon. *High Impulse Voltage and Current Measurement Techniques: Fundamentals, Measuring Instruments, Measuring Method*, Springer International, Jan 2012, p. 195.